

## A Dynamic Model of a Photovoltaic Generator Based on Experimental Data

Maria Carmela Di Piazza, *Member IEEE*, Antonella Ragusa, *Member IEEE*, Massimiliano Luna,  
Gianpaolo Vitale, *Member IEEE*

Consiglio Nazionale delle Ricerche  
Istituto di Studi sui Sistemi Intelligenti per l'Automazione  
(ISSIA – CNR), sezione di Palermo, Via Dante, 12 90141 PALERMO, ITALY  
TEL. +39 091 6113513 FAX +39 091 6113028

[mariacarmela.dipiazza@ieee.org](mailto:mariacarmela.dipiazza@ieee.org), [ragusa@pa.issia.cnr.it](mailto:ragusa@pa.issia.cnr.it), [luna@pa.issia.cnr.it](mailto:luna@pa.issia.cnr.it), [gianpaolo.vitale@ieee.org](mailto:gianpaolo.vitale@ieee.org)

**Abstract.** The aim of this paper is to propose an improvement of a method for the identification of the parameters of photovoltaic (PV) sources model. In a previously published paper the authors developed a single diode model in which characteristic parameters were estimated on the basis of solar radiation by using a robust least squares linear regression (LSR) parameter identification method. In this paper a more accurate temperature estimation is obtained, which includes the dependence on the wind speed. Moreover the dynamic behaviour, both in terms of thermal and electric constants, is considered.

After the description of the adopted methodology a practical case of identification based on measured data is proposed.

### Key words

Models and simulation of renewable energy sources;  
Photovoltaic array; statistics.

### 1. Introduction

Nowadays the study of photovoltaic (PV) sources and the related problems of maximizing the generated power and predicting the plant's behavior in various environmental conditions, is showing a growing interest. Several papers dealing with the PV modeling have been published.

Recently the use of the so called "one diode" model to reproduce the static characteristic I-V has been consolidated [1-8], and it can be successfully obtained both on the basis of data given by manufacturer or obtained experimentally. Such a model can be utilized both for a single cell or PV module and for a whole plant in uniform conditions of solar radiation and temperature.

With such a model it is possible to set up an emulator as in [9, 10] that can be utilized to test power converters topologies and control strategies for photovoltaic sources [11, 12], or to verify the goodness of maximum power point tracking algorithms [13 - 15].

The single diode model parameters depend on cell temperature and solar irradiance, so an accurate knowledge of both of them is necessary. In [6, 16, 17] a model in order to obtain the PV module temperature versus solar irradiance is proposed, in [17] and [18] a

technique to obtain a dynamic model by determining the thermal constant and the equivalent capacitance at the output of the PV generator is described.

This paper proposes an improvement of the model presented in [19] by the same authors. In particular in the latter paper the temperature of the modules was tied only to solar irradiance and the model was static. In order to overcome these limitations a new relationship in which the PV source temperature depends on solar irradiance, wind speed and air temperature has been implemented. Moreover a dynamical model is obtained by evaluating the thermal constant and the electric constant. These results are obtained on the basis of experimental data and by using a robust linear regression to avoid the effect of outliers in the calculus of least squares regressions (LSR).

The paper is organized as follows: in section II a description of the previously developed model of PV module is given; section III gives the fundamentals on the considered linear regressions; several thermal models are presented in section IV; section V deals with the electrical dynamic identification and section VI deals with the thermal dynamic identification; finally in section VII a discussion and the experimental validation are presented.

### 2. PV Source Electrical Model

The I-V curves of the model has been determined in [19]; only the fundamentals are addressed here. The PV cell has a correspondent circuit model reported in fig. 1. Since the presence of the recombination diode is relevant only at low voltage bias, the usual/common simplification of the circuit implements only one diode, so the following I-V equation is obtained [3]:

$$I = I_{ph} - I_s \left( e^{\frac{q(V+IR_s)}{AKT}} - 1 \right) - \frac{V + IR_s}{R_p} \quad (1)$$

If the shunt resistor  $R_p$  is neglected, the well known four parameter model is obtained [2]. This last simplification does not affect significantly the validity of the model. It should be noted that (1) is non-linear and

implicit so its analytical solution is not practicable.

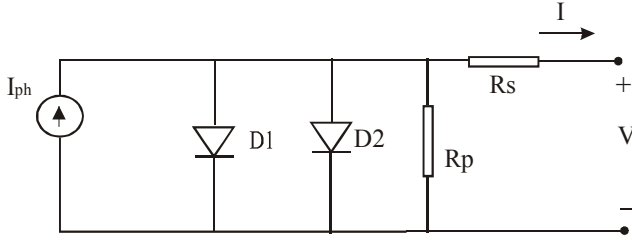


Fig. 1. Equivalent circuit of a PV cell.

This model, developed for a single cell, can be extended to the case of series/parallel connection of PV cells inside a module.

In particular considering  $N_p$  cells in parallel and  $N_s$  cells in series :

$$I_{tot} = N_p I_{ph} - N_p I_s \left( e^{\frac{q}{AKT} \left( \frac{V_{tot} + I_{tot} R_s}{N_s} \right)} - 1 \right) + \frac{V_{tot} + I_{tot} R_s (N_s / N_p)}{R_{sh} (N_s / N_p)} \quad (2)$$

The four parameters model needs four information to be identified. In fact by rewriting for simplicity I-V equation as follows:

$$\begin{cases} I = I_o - e^{[(V+IR_s)K_1+K_2]} \\ \text{where} \\ I_{ph} = I_o; \frac{q}{AKT} = K_1; I_s = e^{K_2} \end{cases} \quad (3)$$

The four parameters to be identified are  $K_1$ ,  $K_2$ ,  $R_s$  and  $I_o$ . They can be obtained by the knowledge of the short-circuit current ( $I_{sc}$ ), the open circuit voltage ( $V_{oc}$ ) and the maximum power point current and voltage ( $I_{mp}$  and  $V_{mp}$ ).

By substituting these parameters into (3) and imposing that the voltage derivative of the power is zero at maximum power point, the model parameters are obtained:

$$\begin{cases} K_1 = \frac{\frac{I_{mp}}{I_o - I_{mp}} + \log[1 - \frac{I_{mp}}{I_o}]}{2V_{mp} - V_{oc}} \\ R_s = \frac{V_{mp} - \frac{I_{mp}}{[I_o - I_{mp}]K_1}}{I_{mp}} \\ K_2 = \log[I_o] - V_{oc}K_1 \\ I_{sc} = I_o - e^{(I_{sc}R_s)K_1+K_2} \end{cases} \quad (4)$$

The last equation has the form  $I_{sc}=f(I_{sc})$  and it could be solved by an iterative method; however the contribution of the exponential term is negligible because it contains a coefficient that corresponds to a reverse saturation current; as a consequence it can be assumed  $I_{sc} = I_o$ . It should be noticed that the obtained value of  $R_s$  takes into

account the connecting cables resistance if  $I_{mp}$  and  $V_{mp}$  are measured directly on the load.

As for the knowledge of  $I_{sc}$  and  $V_{oc}$ , they are usually given by the manufacturer under standard test conditions, i.e. AM1.5, corresponding to a solar irradiance  $G_{stc}=1000$  W/m<sup>2</sup> and a cell temperature  $T_{stc}=25$  °C. Their values for each values of solar irradiance,  $G$ , and temperature,  $T$ , can be determined considering the following expressions,

$$\begin{cases} V_{oc} = V_{oc(stc)} + \Delta V_T (T - T_{stc}) \\ I_{sc} = \frac{G}{G_{stc}} I_{sc(stc)} \end{cases} \quad (5)$$

where  $V_{oc(stc)}$  and  $I_{sc(stc)}$  are the open circuit voltage and the short circuit current given by manufacturer under standard test conditions and  $\Delta V_T = -0.08$  V/°C for the case under study. It should be noted that the  $V_{oc}$  variation depends (weakly) on the temperature, on the contrary irradiance has a large effect on short circuit current.

It is also possible to achieve the values of  $V_{oc}$  and  $I_{sc}$  through off line measurements on the PV plant. The  $V_{oc}$  can be obtained by a voltage measurement without the inverter; the measure of  $I_{sc}$  is more difficult because it requires the short circuit condition. However by performing some measurement also the coefficients of (3) can be deduced.

As for  $V_{mp}$ ,  $I_{mp}$ , they could be deduced by data logger.

In the case under study the data logger acquires data each 10 minutes, the voltage and current when the inverter is running should correspond to  $V_{mp}$ ,  $I_{mp}$ .

By measuring data it is possible to obtain informations about the real characterization of the plant, including the series resistance represented by the cables that connect the photovoltaic generator to the inverter. To this aim it is necessary to manage data in order to discriminate the “noise” represented by undesired measurements.

In [19] the  $V_{mp}$ ,  $I_{mp}$  values versus solar irradiance and temperature have been obtained through a robust linear regression. This is justified because the dispersion diagram of T versus G exhibits a linear trend with some outliers. The use of robust regression allows to avoid a bias in the straight curve.

With the robust LSR, the following equations for  $I_{mp}$  and  $V_{mp}$  have been obtained:

$$\begin{cases} I_{mp} = -0.470 + 0.0071G \\ V_{mp} = 172.440 - 0.0115G \end{cases} \quad (6)$$

### 3. Linear Regressions

It is often necessary to obtain a mathematical relation between two (or more) variables. If  $(X_1, X_2, \dots, X_N)$  and  $(Y_1, Y_2, \dots, Y_N)$  are two set of data, by drawing the couples  $(X_i, Y_i)$  in a Cartesian diagram, a so-called dispersion diagram is obtained. In such a diagram, if it is possible to identify a curve that approximates the drawn data, the curve is said interpolating curve.

The problem consists on the choice of the curve and on the calculus of its parameters. The simplest curve is the straight line. In formulas, the interpolating straight

line may be written as:

$$Y = a_0 + a_1 X \quad (7)$$

The equation (7) estimates the variable  $Y$  on the basis of the value of the variable  $X$ , the line is said regression curve of  $Y$  on  $X$ . In order to find a good approximation, the coefficients  $a_0, a_1$  can be chosen so to minimize the sum of the square of the distance between each point  $(X_i, Y_i)$  and the line obtaining the least square straight line. The least square minimization may be also utilized with other kinds of curves.

When more than two variables are involved, a similar approach can be utilized; for example among three variables  $X, Y$  and  $Z$  a linear regression gives a plane:

$$Z = h_0 + h_1 X + h_2 Y \quad (8)$$

and the use of more complicated regression surfaces can be investigated.

A measure of the fitting goodness of the data on the considered curve is given by the correlation coefficient and by the standard error. The correlation coefficient value can vary in the range  $-1$  and  $+1$ ; if the value is zero there is not any linear correlation between the two variables  $X$  and  $Y$ .

It is common, especially when data come from measurement, the presence of outliers. In such a case the traditional LSR can be affected by inaccuracy.

Robust regression is a form of regression analysis devised to overcome some limitations of traditional regression methods.

The application of the robust regression method for the PV model parameters identification is performed within Matlab® environment. In particular the embedded *robustfit* function is used to obtain the regression straight line coefficients estimates.

The *robustfit* function uses an iteratively re-weighted least squares algorithm, with the weights at each iteration calculated by applying the bisquare function to the residuals from the previous iteration. This algorithm gives lower weight to points that do not fit well. The results are less sensitive to outliers in the data as compared with ordinary LSR [20-22].

#### 4. The thermal model

In [16] the photovoltaic modules temperature was obtained versus solar radiation through a linear LSR. This approach was based on the consideration that the dispersion diagram of  $T$  versus  $G$  exhibited a linear trend.

Several thermal models have been proposed in literature with the aim to obtain the module's temperature versus solar irradiation, air temperature and wind speed. The simplest is described in [13] in which the temperature has a linear dependence on irradiance, air temperature and wind speed as in eq. (9).

$$T_{mod} = a_1 \cdot T_{amb} + a_2 \cdot G + a_3 \cdot W + a_4 \quad (9)$$

Where  $T_{mod}$  is the temperature of the module in °C,  $T_{amb}$

is the environmental temperature in °C,  $G$  is the solar irradiation in Watt/m<sup>2</sup> and  $W$  is the wind speed in m/s. In (9)  $a_1 \approx 1$ , it means that  $T_{mod} \approx T_{amb}$  with no solar radiation and wind.

In [13] a more complicated model is proposed according to eq (10):

$$T_{mod} = T_{amb} + (b_1 + b_2 \cdot W + b_3 \cdot W^2) + G(b_4 + b_5 \cdot W + b_6 \cdot W^2) \quad (10)$$

In [17] and [18], in order to take into account the site dependent influences and anemometer installations different from standard meteorological practice, a non linear relationship is used. This tuning is achieved through two coefficients ( $a, b$ ) which can be determined analyzing data recorded after system installation.

$$T_{mod(bs)} = G \{ \exp(a + b \cdot W) \} + T_{amb} \quad (11)$$

where  $T_{mod(bs)}$  = Back-surface module temperature, (°C).

$a$  = Empirically-determined coefficient establishing the upper limit for module temperature at low wind speeds and high solar irradiance;

$b$  = Empirically-determined coefficient establishing the rate at which module temperature drops as wind speed increases.

The back surface temperature can be related with the module temperature assuming an one-dimensional thermal heat conduction through the module materials behind the cell (encapsulant and polymer layers for flat-plate modules, ceramic dielectric and aluminum heat sink for concentrator modules) as in (12),

$$T_{mod} = T_{mod(bs)} + \frac{G}{G_{stc}} \Delta T \quad (12)$$

in which  $\Delta T$  is temperature difference between the cell and the module back surface at an irradiance level of 1000 W/m<sup>2</sup>. This temperature difference ranges typically from 2 to 3 °C for flat-plate modules in an open-rack mount. For flat-plate modules with a thermally insulated back surface, this temperature difference can be assumed to be zero. For concentrator modules, this temperature difference is typically determined between the cell and the root of a finned heat exchanger (heat sink) on the back of the module. Several values of  $\Delta T$  used to predict module back surface temperature as a function of irradiance, ambient temperature, and wind speed are reported in [18].

Despite of non linearity, in (11) the  $a$  and  $b$  coefficients, could be achieved through a LSR; as a matter of fact (11) can be rewritten as:

$$\ln \left( \frac{T_{mod(bs)} - T_{amb}}{G} \right) = a + b \cdot W \quad (13)$$

A linear regression can be performed to fit the data providing the coefficients ( $a$ ,  $b$ ) for the thermal model.

In [18] several couples of ( $a$ ,  $b$ ) are provided too. Moreover, it should be noted that (11) can be rewritten as:

$$\begin{aligned} T_{\text{mod}(bs)} &= G\{\exp(a) \cdot \exp(b \cdot W)\} + T_{\text{amb}} = \\ &= c_1 G \exp(b \cdot W) + T_{\text{amb}} \approx c_1 G(1 - b \cdot W) + T_{\text{amb}} = \\ &= c_1 G + c_2 GW + T_{\text{amb}} \end{aligned} \quad (14)$$

where  $c_1 = \exp(a)$  and  $c_2 = -c_1 \cdot b$ . This last expression is equivalent to (10) when  $b_3 \ll b_2$  and  $b_6 \ll b_5$ .

## 5. Electric constant identification

The electric dynamic behaviour of a PV module can be represented by an equivalent capacitance parallel connected to the output of the “one diode model” as shown in fig 2 [17].

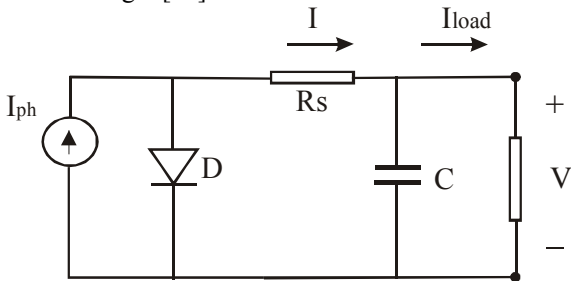


Fig. 2. Equivalent circuit of a PV cell with the internal capacitance.

With the capacitance  $C$  the output voltage derivative is given by:

$$\frac{\partial V}{\partial t} = \frac{1}{C} [I(V) - I_{\text{load}}] \quad (15)$$

by measuring during a suitable transient  $I_{\text{load}}$  and the voltage derivative and utilizing the model for achieving the correspondent values of  $I(V)$ , the value of  $C$  can be achieved through a linear regression.

## 6. Thermal constant identification

In section 4 thermal models have been discussed. All the described models do not take into account the temperature time variation. However a comprehensive analysis must consider thermal dynamic too. The change of the temperature is well described by a first order system [17] so the temperature variation can be expressed as:

$$\frac{dT}{dt} = -\frac{1}{\tau_{\text{th}}} (T - T_{\text{ss}}) \quad (16)$$

where  $T_{\text{ss}}$  is the steady state temperature and  $\tau_{\text{th}}$  is the thermal time constant. Also in this case on the base of a suitable measured thermal transient, a linear regression allows to identify  $\tau_{\text{th}}$ .

## 7. Discussion and Experimental Validation

The following analyses have been performed on a test rig which is composed of a set of two p-Si PV modules with the same following reference values:

$P_N=5$  W<sub>p</sub>,  $V_{OC}=21,6$  V,  $I_{SC}=0.43$  A,  $V_{mp}=17,2$  V,  $I_{mp}=0.39$  mA at standard test conditions AM1.5 1000W/m<sup>2</sup>, 25 °C. The modules are mounted on a frame which is tilted at 50°, facing South, and they are connected to an electronic board which allows to switch among different values of load resistors (24 Ω, 47,5 Ω, 3260 Ω and no load) to test the corresponding operating points.

The four parameters ( $V_{OC}$ ,  $I_{SC}$ ,  $V_{mp}$ ,  $I_{mp}$ ) of the modules are known for values of the solar radiation  $G$  in the range 640÷870 W/m<sup>2</sup>.

### A. Module temperature estimation

A measurement campaign was performed from the beginning of June to the end of August. The following parameters were sampled hourly: module temperature, air temperature, solar radiation and wind speed. Each vector contains 2160 samples. In figure 3 the difference between the module temperature and the air temperature is drawn versus the solar radiation and wind speed. It should be noted that these data are distributed around a plane.

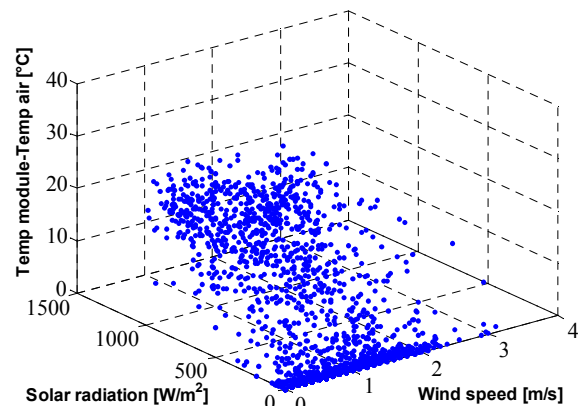


Fig. 3: plot of the difference between the module temperature and the air temperature versus solar radiation and wind speed.

It is reasonable to perform a LSR in order to obtain the module temperature versus solar radiation, wind speed and air temperature according to the equation:

$$T = \alpha_1 G + \alpha_2 W + \alpha_3 T_{\text{amb}} \quad (17)$$

The LSR gives the following coefficients:  $\alpha_1=0.0224$ ,  $\alpha_2=-0.7027$ ,  $\alpha_3=1.0078$

The corresponding interpolating plane is drawn in fig. 4 superimposed on the sampled data.

The  $a$  and  $b$  coefficients of the (11) could be obtained through a linear regression on (13), however in this case a preprocessing of data it is necessary in order to eliminate the values that correspond to  $T_{\text{amb}} \approx T_{\text{mod}}$  and  $G \approx 0$  that introduce singularities.

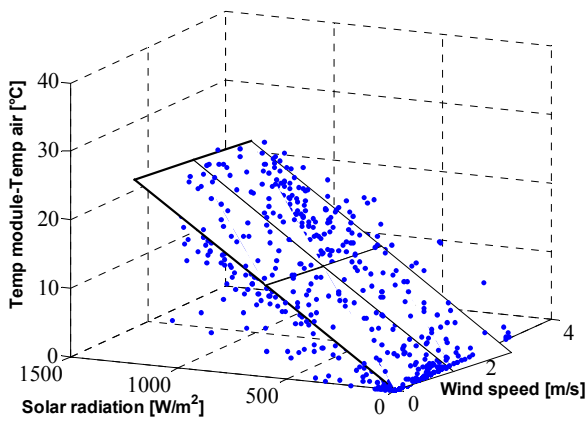


Fig. 4: interpolating plane and sampled data

By utilizing (14) and performing a LSR on the solar radiation, the product of the solar radiation and wind speed and air temperature the following equation is obtained:

$$T = \beta_1 G + \beta_2 GW + \beta_3 T_{amb} \quad (18)$$

with the coefficients:  $\beta_1=0.0256$ ,  $\beta_2=-0.0030$ ,  $\beta_3=0.986$ , from which:

$$\begin{cases} a = \log \beta_1 = -3.66 \\ b = \frac{\beta_2}{-e^a} = 8.1967 \cdot 10^{-4} \end{cases}$$

Fig. 5 shows the quantity  $\log((T_{mod}-T_{air})/G)$  versus the wind speed with the interpolating line  $y=a+bx$  superimposed. It should be noted that the  $a$  coefficient is coherent with [18] and experimental data but the  $b$  coefficient suffers of a poor data preprocessing.

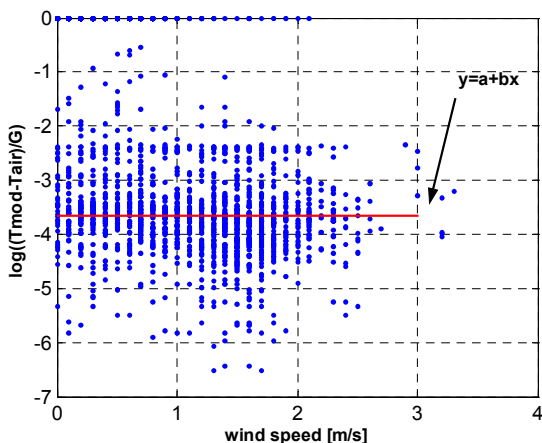


Fig. 5:  $\log((T_{mod}-T_{air})/G)$  versus the wind speed with the interpolating line  $y=a+bx$  superimposed.

### B. Equivalent capacitance evaluation

By means of an Agilent MSO6104A 4 Gsamples/s scope, the waveforms of load voltage and load current have been acquired during the transient from the open circuit point ( $R_{LOAD} \rightarrow \infty$ ) to the maximum power point ( $R_{LOAD}=47,5 \Omega$ ). The test has been carried out at noon in

a clear day, in order to work with a constant value of the solar radiation. A pyranometer Kipp&Zonen CM6b, installed with the same tilt as the modules, has given a value of  $G=738 \text{ W/m}^2$ , at which the characteristic parameters of the modules are:  $V_{OC}=18,4 \text{ V}$ ,  $I_{SC}=0.29 \text{ A}$ ,  $V_{mp}=13,5 \text{ V}$ ,  $I_{mp}=0.26 \text{ A}$ . By substituting these values in the set of equations (4), the four parameters of the model described by equation (3) have been found:

$$I_0=0.292 \text{ A}, R_S=6.48 \Omega, K_1=0.6876, K_2=-13.88. \quad (19)$$

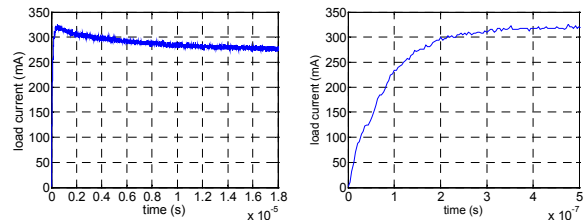


Fig. 6: a) current transient, b) initial part of the current transient.

Figure 6a shows the load current waveform, in fig 6b the initial part of the same transient is reported. The overshoot in the waveform of fig. 6a suggests that the first order equivalent circuit of figure 2 is not suitable to model the behaviour of the system; instead, a series inductor, mainly due to the connecting cables, should be added before the load resistor, as shown in figure 7. The absence of the inductor in the model implies that the load voltage would be equal to the module voltage, and that would lead to an absurd: when the module voltage decreases from  $V_{OC}$  to its final value  $V(\infty)$ , the load current would decrease from  $V_{OC}/R_{LOAD}$  to its final value  $I(\infty)=V(\infty)/R_{LOAD}$  instead of increasing from zero to  $I(\infty)$ , and also the load voltage would have this erroneous decreasing trend. Hence only adding an inductor the transient of fig. 6b is correctly reproduced.

The waveform of figure 6a, just as in any RLC circuit, can be considered as the sum of a constant and two curves which are not true exponentials because of the nonlinearity of the PV generator.

However the initial parts of these curves are very close to exponentials, since during this time interval the module voltage falls to a value which is not so different from the open circuit voltage and the operating point moves in a portion of the characteristic which is nearly linear.

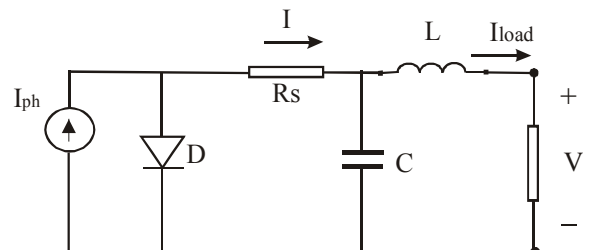


Figure 7. The complete electric equivalent circuit

In addition, the effects of the inductor (front edge of the signal, fig 6b) and of the capacitor (trailing tail of the waveform) are clearly distinct, since the two time constants  $\tau_L=(L/R_{LOAD})$  and  $\tau_C=R_{LOAD} \cdot C$  are more than

one order of magnitude different, as the final results will show. This allows to say that the front edge is given by the inductive exponential alone and that just a part of the trailing tail which starts a bit after the peak has a capacitive exponential trend, being the subsequent part distorted because of the nonlinearity.

If the PV source were linear the load current would be given by the following formula:

$$I_{LOAD,lin} \cong -\frac{V_{OC}}{R_{LOAD}} e^{-\frac{t}{\tau_L}} + \left( \frac{V_{OC}}{R_{LOAD}} - I_{LOAD,lin}(\infty) \right) e^{-\frac{t}{\tau_C}} + I_{LOAD,lin}(\infty) \quad (20)$$

The (20) can be rearranged so to put in evidence:

$$I_{LOAD,lin} = I_1 + I_2 + K$$

where:

$$I_1 = \frac{V_{OC}}{R_{LOAD}} \left( 1 - e^{-\frac{t}{\tau_L}} \right) \quad (21a)$$

$$I_2 = \left( \frac{V_{OC}}{R_{LOAD}} - I_{LOAD,lin}(\infty) \right) e^{-\frac{t}{\tau_C}} + I_{LOAD,lin}(\infty) \quad (21b)$$

$$K = -\frac{V_{OC}}{R_{LOAD}} \quad (21c)$$

The previous considerations allow the identification of the parameters L and C by means of a linear regression of the natural logarithm of suitable portions of the load current or voltage. The load current is a preferred choice since, being equal to the inductor current, it is a state variable.

If the peak time is referred to as  $t^*$  and  $\Delta t$  corresponds to a convenient portion of waveform after the peak, despite the nonlinearity it is possible to say that:

$$\begin{cases} I_{LOAD}|_0^{t^*-\varepsilon} = I_1|_0^{t^*-\varepsilon} \\ I_{LOAD}|_{t^*+\varepsilon}^{t^*+\varepsilon+\Delta t} = I_2|_{t^*+\varepsilon}^{t^*+\varepsilon+\Delta t} \end{cases} \quad (23)$$

where  $\varepsilon$  is a suitable non zero quantity and  $I_{LOAD}$  is the actual load current. Therefore, in order to identify the inductance value, it is possible to apply LSR to the logarithm of the (21a) rewritten as:

$$e^{-\frac{t}{\tau_L}} = 1 - \frac{R_{LOAD}}{V_{OC}} I_{LOAD}|_0^{t^*-\varepsilon} = 1 - \frac{1}{V_{OC}} V_{LOAD}|_0^{t^*-\varepsilon} \quad (24)$$

The opposite of the angular coefficient will give the inverse of the time constant and the inductance will be given by  $L = \tau_L \cdot R_{LOAD}$ . Using the acquired data shown in figure 6b, the value  $L = 5.4 \mu\text{H}$  has been found.

Similarly, in order to identify the capacitance value it

is possible to apply a LSR to the logarithm of the (21b) rewritten as:

$$e^{-\frac{t}{\tau_C}} = \frac{I_{LOAD}|_{t^*+\varepsilon}^{t^*+\varepsilon+\Delta t} - I_{LOAD,lin}(\infty)}{\frac{V_{OC}}{R_{LOAD}} - I_{LOAD,lin}(\infty)} \quad (25)$$

The opposite of the angular coefficient will give the inverse of the time constant and the capacity will be given by  $C = \tau_C / R_{LOAD}$ . Using the acquired data shown in figure 6a, the value  $C = 130.6 \text{ nF}$  has been found.

Figures 8a and 8b show respectively parts of the front edge and of the trailing tail of the waveform, plotted on semilog graphs, with their regression lines superimposed.

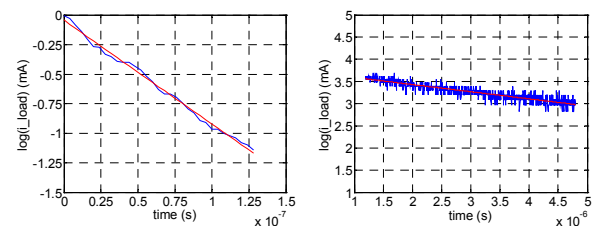


Figure 8: a) front edge of the waveform on a semilog graph, b) trailing tail of the waveform on a semilog graph

### C. Thermal constant evaluation

In order to utilize (16) a thermal transient has been acquired. A temperature transient was sampled with a solar radiation of  $1100 \text{ W/m}^2$  in absence of wind. One sample every 132 s was memorized; the transient has a duration of about 8000 s.

By using a LSR on  $dT/dt$  and  $T - T_{ss}$  a value of  $-0.0012$  is obtained for the coefficient. It corresponds to  $\tau = 852.9 \text{ s}$ .

In fig. 9 the sampled transient and the curve obtained by solving (16), where  $\tau$  is obtained through LSR, are shown. The estimation is less accurate in the first part of the transient due to the use of the temperature derivative.

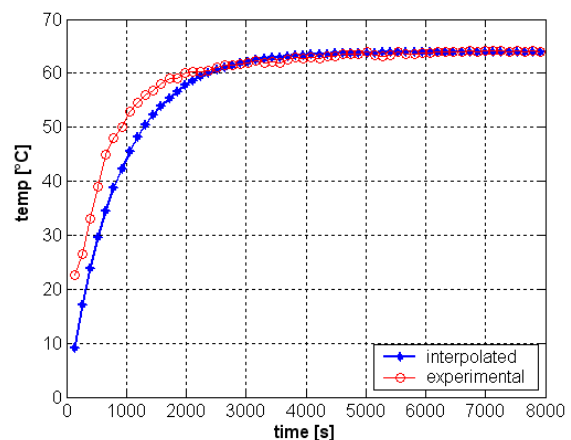


Fig. 9. thermal transient: experimental and interpolated data.

## 8. Conclusions

In this paper an improvement of a previously set up PV source model is proposed, with the parameters identification based on a robust LSR method. The module temperature is obtained versus solar radiation and wind speed. The electrical and thermal constants are identified.

An overview of the methods presented in the literature is reported and the difficulties which arise by using experimental data are highlighted with reference to a practical case study.

## References

- [1] J.A. Gow, C.D. Manning, "Development of a photovoltaic array model for use in power electronics simulation studies", IEE Proc. Electronic Power Applications, Vol.146, No. 2, Mar. 1999, pp.193 – 200.
- [2] W. Xiao, W.G. Dunford, A. Capel, "A novel modeling method for Photovoltaic cells", in Proc. IEEE 35th Annual Power Electron. Spec. Conf., Aachen, Germany, 2004, pp.1950 – 1956.
- [3] Yamashita, H.; Tamahashi, K.; Michihira, M.; Tsuyoshi, A.; Amako, K.; Park, M., "A novel simulation technique of the PV generation system using real weather conditions", in Proc. Power Conversion Conf., Apr.-2-5, 2002, pp.839-844.
- [4] D. Sera, R. Teodorescu, P. Rodriguez, "PV panel model based on datasheet values", *IEEE International Symposium on Industrial Electronics ISIE 07*, June 4-7, 2007, pp.2392-2396.
- [5] R. Chenni, M.Makhlouf, T.Kerbache, A.Bouزيد, "A detailed Modeling for Photovoltaic Cells", *Elsevier, Energy 32, 2007*, pp.1724-1730.
- [6] G.M. Tina, S. Scorfani, "Electrical and Thermal Model for PV Module Temperature Evaluation", *Electrotechnical Conference, 2008. MELECON 2008. The 14th IEEE Mediterranean 5-7 May 2008* Page(s): 585 – 590
- [7] Ryan C. Campbell, A Circuit-based Photovoltaic Array Model for Power System Studies, *Power Symposium, 2007. NAPS '07. 39th North American*, Sept. 30 2007-Oct. 2 2007 Page(s):97 – 101.
- [8] Tomáš Skočil, Manuel Pérez Donsión, "Mathematical Modeling and Simulation of Photovoltaic Array", *International Conference on Renewable Energy and Power Quality 2008 (ICREPO08)*, Santander (Spain) 12-14 march 2008. Online available <http://www.icrepq.com/papers-icrepq08.htm>
- [9] M. Cirrincione, M. C. Di Piazza, G. Marsala, M. Pucci, G. Vitale "Real Time Simulation of Renewable Sources by Model-Based Control of DC/DC Converters", *IEEE International symposium on Industrial Electronics, ISIE 2008*, 29 June 2 July 2008, Cambridge, UK.
- [10] M.C. Di Piazza, G. Vitale, "Photovoltaic field emulation including dynamic and partial shadow conditions", *Applied Energy*, available on-line 29 oct 2009, DOI information: 10.1016/j.apenergy.2009.09.036
- [11] P.Sanchis, I. Echeverria, A. Ursua, O. Alonso, E. Gubia, L. Marroyo, "Electronic converter for the analysis of photovoltaic arrays and inverters", in *Proc. IEEE 34<sup>th</sup> Power Electron. Spec. Conf.*, vol. 4, 15-19 Jun. 2003, pp.1748-1753.
- [12] Il-Song Kim, Sliding mode controller for the single-phase grid-connected photovoltaic system, *Applied Energy*, 83 (2006) 1101–1115.
- [13] Matsukawa H, Koshiishi K, Koizumi H, Kurokawa K, Hamada M, Bo L. Dynamic evaluation of maximum power point tracking operation with PV array simulation. *Sol Energy Mater Sol Cells* 2003;75:537–46
- [14] M. I. Arteaga Orozco, J. R. Vázquez, P. Salmerón, S. P. Litrán, F. J. Alcántara, "Maximum power point tracker of a photovoltaic system using sliding mode control", *International Conference on Renewable Energies and Power Quality (ICREPO'09) Valencia (Spain)*, 15th to 17th April, 2009. Online available <http://www.icrepq.com/papers-icrepq09.htm>
- [15] P. C. M. Bernardo1, Z. M. A. Peixoto and L.V. B. Machado Neto, "A High Efficient Micro-controlled Buck Converter with Maximum Power Point Tracking for Photovoltaic Systems", *International Conference on Renewable Energies and Power Quality (ICREPO'09) Valencia (Spain)*, 15th to 17th April, 2009. Online available <http://www.icrepq.com/papers-icrepq09.htm>
- [16] G. TamizhMani, L. Ji, Y. Tang, L. Petacci, C. Osterwald "Photovoltaic Module Thermal/Wind Performance: Long - Term Monitoring and Model Development For Energy Rating" NCPV and Solar Program Review Meeting 2003 NREL/CD-520-33586 Page 936
- [17] Omar Gil-Arias, Eduardo I. Ortiz-Rivera, "A General Purpose Tool for Simulating the Behavior of PV Solar Cells, Modules and Arrays", *Control and Modeling for Power Electronics, 2008. COMPEL 2008. 11th Workshop on 17-20 Aug. 2008* Page(s):1 – 5.
- [18] D. L. King, W. E. Boyson, J. A. Kratochvil "PHOTOVOLTAIC ARRAY PERFORMANCE MODEL" Sandia National Laboratories Albuquerque, New Mexico 87185-0752.
- [19] A. Ragusa, M. C. Di Piazza, G. Vitale, "Identification of Photovoltaic Array Model Parameters by Robust Linear Regression Methods", *International Conference on Renewable Energy and Power Quality 2009 (ICREPO09)*, Valencia (Spain) 15-17 april 2009. Online available <http://www.icrepq.com/papers-icrepq09.htm>
- [20] Holland, P.W., and R.E. Welsch (1977), "Robust Regression Using Iteratively Reweighted Least-Squares," *Communications in Statistics: Theory and Methods*, A6, pp.813-827.
- [21] Huber, P.J. (1981), *Robust Statistics*, New York: Wiley.
- [22] Street, J.O., R.J. Carroll, and D. Ruppert (1988), "A Note on Computing Robust Regression Estimates via Iteratively Reweighted Least Squares," *The American Statistician*, 42, pp.152-154.